ISBN: 978-3-95450-211-0 doi:10.18429/JACoW-SRF2019-TUP037

CONSTRUCTION OF SUPERCONDUCTING LINAC BOOSTER FOR HEAVY-ION LINAC AT RIKEN NISHINA CENTER

K. Yamada*, T. Dantsuka, H. Imao, O. Kamigaito, K. Kusaka, H. Okuno, K. Ozeki, N. Sakamoto, K. Suda, T. Watanabe, Y. Watanabe, RIKEN Nishina Center, Wako, Saitama, Japan
E. Kako, H. Nakai, H. Sakai, K. Umemori, KEK, Tsukuba, Ibaraki, Japan
H. Hara, A. Miyamoto, K. Sennyu, T. Yanagisawa,
Mitsubishi Heavy Industries Machinery Systems, Ltd. (MHI-MS), Kobe, Hyogo, Japan

Abstract

The RIKEN Heavy-Ion Linac is undergoing an upgrade of its acceleration voltage in order to enable it for further investigations of new super-heavy elements and radioactive isotope production. In this project, a new superconducting booster linac is being developed and constructed. The booster linac consists of 10 TEM quarter-wavelength resonators made of pure niobium which operate at 4.5 K. The target performance of each resonator is $Q_0 = 1 \times 10^9$ with an accelerating gradient of 6.8 MV/m. We succeeded in developing high-performance resonators which satisfy the requirements with a wide margin. The cryomodule assembly and installation of the cryomodules and a helium refrigerator system were completed by the end of FY2018. A cooling-down test is scheduled for September 2019. This article reports the construction status of the superconducting booster linac.

INTRODUCTION

The existing heavy-ion linac, RILAC [1], at the RIKEN Nishina Center plays an important role of supplying intense beams for the synthesis of super-heavy elements (SHEs) as well as acting as the injector for the succeeding RIKEN Ring Cyclotron. The RILAC has been in operation since 1982 and was originally designed to have a total acceleration voltage of 16 MV with six drift-tube-linac (DTL) tanks. Each DTL tank is a room-temperature (RT) quarter-wavelength resonator (QWR) which can vary its resonant frequency from 17 to 45 MHz. For example, the original RILAC can accelerate heavy-ions with a mass-to-charge ratio (m/q) of 6 up to 2.7 MeV/u with 36.5 MHz operation. In 1996, the front end of the RILAC was replaced by an 8 GHz electron-cyclotron-resonance ion source (ECRIS) with a 500 kV Cockcroft–Walton electrostatic accelerator connected to an 18 GHz ECRIS and a variable frequency RFQ linac [2] to increase the beam intensity. Six new DTL tanks (A1–6), with a resonant frequency twice that of the RILAC, were added downstream of the RILAC as a booster linac [3] in 2001 to increase the beam energy for SHE synthesis experiment, etc. Synthesis experiments on the 113th element started in 2003 using a $^{70}Zn^{14+}$ beam with an energy of 5 MeV/u accelerated by the RILAC and a booster with frequencies of 37.75 MHz and 75.5 MHz, respectively. The first synthesis of element 113 was achieved in July 2004 [4]. The 113th element, nihonium, named for Japan, was listed in the periodic table in November 2016, and the seventh period of the table was completed by the determination of the names up to element 118 at the same time.

Recently, we proposed an upgrade project [5] to increase the beam intensity and energy of the RILAC, aimed at making possible SHE experiments for the eighth period of the table, as well as producing valuable radioactive isotopes. It was planned that the beam intensity would be increased dramatically by introducing a new 28 GHz superconducting (SC) ECR ion source [6] at the front end of the RILAC. We removed the last four tanks of the booster linac, A3–6, and installed an SC booster linac (SRILAC) consisting of 10 SC-QWRs to boost the beam energy to over 6.5 MeV/u for heavy ions with $m/q = 6$. The full layout plan of the SRILAC is shown in Fig. 1.

Construction of the SRILAC started in the autumn of 2016 when the budget was finalized. Figure 2 shows the construction schedule of the SRILAC. The status of the construction is reported in this paper. The status up to 2018 was reported in Ref. [7].

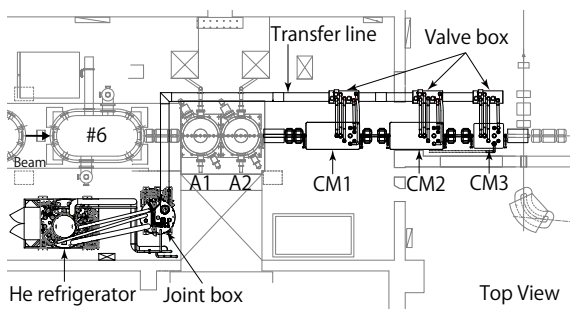

Figure 1: Full layout plan of the SRILAC.

SUPERCONDUCTING BOOSTER LINAC

Outline

The 10 SC-QWRs of the SRILAC are arranged into groups of 4 units, 4 units, and 2 units, stored in three cryomodules (CM1–3). The resonant frequency of the SC-QWR was chosen to be 73 MHz, twice the fundamental frequency of the RF system of the RIKEN Radioactive Isotope Beam Factory (RIBF) [8,9] accelerators. The geometry of the SC-QWRs is optimized for $\beta_{opt} = 0.078$, which is almost compatible with the beam energy of 3.61 MeV/u at the exit of the A2 tank for 73.0 MHz operation. The operation temperature is 4.5 K, using a Claude-cycle liquid-helium refrigerator located in the vicinity of the cryomodules. We adopted an RT quadrupole

* nari-yamada@riken.jp

ISBN: 978-3-95450-211-0 doi:10.18429/JACoW-SRF2019-TUP037

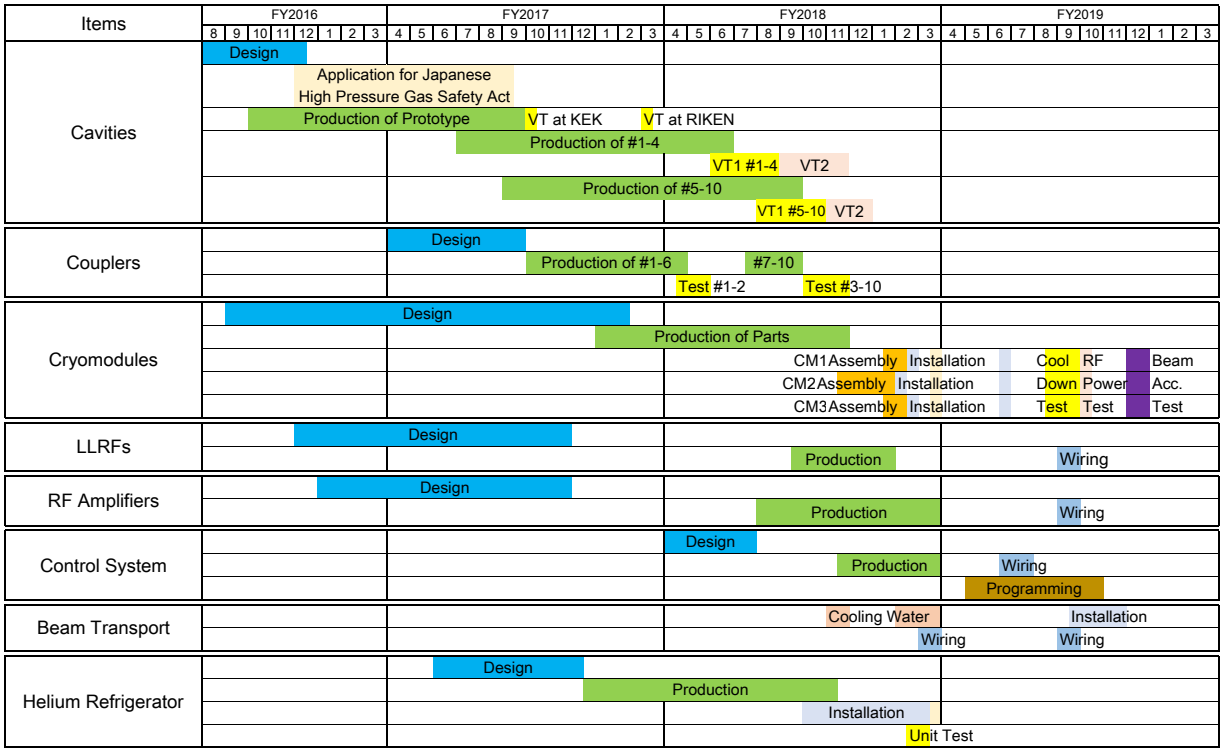

Figure 2: Construction schedule of the SRILAC.

doublet for the focusing element between the cryomodules as well as in front and at the end of the SRILAC. The fundamental design of the SC-QWRs, cryomodule, and lattice is based on the SC part of the upgrade plan [10–12] for the RIBF, which was conceptually designed in 2013 and optimized in 2014. The fabrication technology of the SC-QWRs and cryomodule had already been developed by prototyping [13–15] as a part of the ImPACT program [16]. The designed gap voltage was raised from 0.8 MV to 1.2 MV due to the good results of performance tests of the first prototype. The design parameters of the SC-QWRs are listed in Table 1. Here, the effective length for obtaining E_{acc} is set to $\beta_{opt}\lambda = 0.32$ m.

Table 1: Design Parameters of the SC-QWRs for the SRILAC. The surface resistance is conservatively assumed to be 22.4 nΩ in the calculation.

Frequency [MHz] at 4.5 K	73.0
Duty [%]	100
β_{opt}	0.078
Aperture [mm]	ϕ40
G [Ω]	22.4
R_{sh}/Q_0 [Ω]	579
Q_0	1.0×10^9
P_0 [W]	8
V_{acc} [MV] at E_{acc} = 6.75 MV/m, β = 0.078	2.16
E_{acc} [MV/m]	6.75
E_{peak}/E_{acc}	6.2
B_{peak}/E_{acc} [mT/(MV/m)]	9.6

Fabrication of SC-QWRs

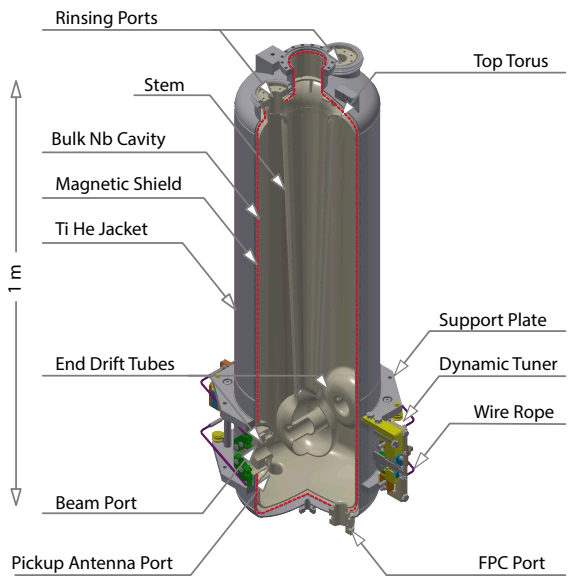

Figure 3: Schematic of a SC-QWR for the SRILAC.

Figure 3 shows a schematic of an SC-QWR. The SC-QWRs are made from pure niobium sheets with a residual resistance ratio of 250, and are contained within a helium jacket made of pure titanium. The niobium sheets were machined, press-formed, and electron beam welded (EBW) with port parts manufactured by cutting a niobium round bar to form four partial components, a stem, a top torus, an outer cylinder, and a bottom dome, as shown in Fig. 4. The

ISBN: 978-3-95450-211-0 doi:10.18429/JACoW-SRF2019-TUP037

thicknesses of the stem and upper side of the outer cylinder are 3.5 mm and 4 mm. The number of ports was cut from nine in the first prototype to six to reduce the fabrication cost. The flanges of each port and the ribs are made from grade 2 hard niobium. Tin-plated U-TIGHTSEAL is used for the vacuum sealing for each port, and the flanges are tightened with NC25 copper alloy bolts. A rib structure on the top torus was optimized to reduce the influence of microphonics and to suppress the deformation due to fluctuations of the helium pressure. Frequency tuning of the SC-QWRs was realized by compressing beam ports in the direction of the beam axis. The compression force is driven by decelerating the rotational force of the stepping motor with reduction gears and pulling a wire wound around the cavity, converting the pulling force into displacement in the beam axial direction. The shape around the end drift tube was optimized to reduce the maximum stress to less than 90 MPa, required to comply with the High-Pressure Gas Safety Act in Japan. A magnetic shield was installed between the bulk SC-QWR and the jacket for shielding performance and ease of cryomodule assembly. After the production of the partial components, the resonant frequency of their assembly was measured and carefully adjusted step by step by cutting the straight section between the top torus, stem, and outer cylinder, as well as the outer cylinder and bottom dome. Details of the frequency adjustment and SC-QWR fabrication are described in Ref. [17].

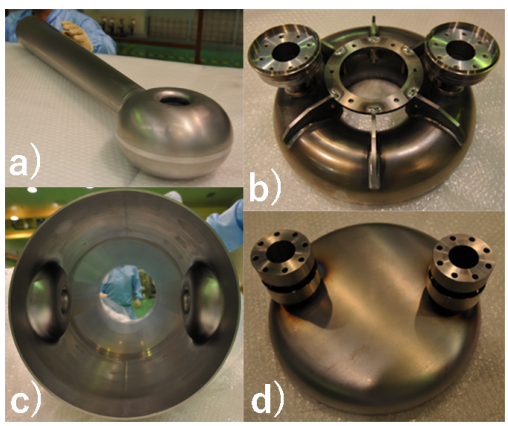

Figure 4: Photographs of the stem (a), top torus (b), inner view of outer cylinder (c), and bottom dome (d) of an SC-QWR.

A second prototype bulk SC-QWR was produced to validate the modified design and prepare the jigs and manufacturing parameters before we started making the final SC-QWRs. After the validation of the prototype resonator, ten bulk SC-QWRs were fabricated and processed with an inner surface treatment. The surface treatment consisted of a sequence of treatments [18]: 110 µm buffered chemical polishing (BCP), ultrasonic cleaning with pure water, annealing at 750 °C for 3 hours, 20 µm BCP, ultrasonic cleaning with detergent, rinsing by pure water, high-pressure rinsing (HPR) with 8 MPa ultra-pure water, and baking at 120 °C for 48 hours. Pre-tuning [17] of the resonant frequency and a pressure test to comply with safety regulations were performed before the second BCP. Assembly after the HPR was performed in an ISO class 1 clean room (KOKEN floor KOACH) at the factory of a private company.

We prepared a test stand at the RIKEN based on the test stand at KEK [14] to confirm whether an acceptable performance could be obtained for each SC-QWR. We drilled a hole in the floor and installed a cryostat with an inner diameter of 700 mm and a depth of 3240 mm. A magnetic shield was put into the cryostat to prevent the penetration of geomagnetism and a value of less than 10 mGauss was achieved. An input coupler for the vertical test was designed with a stroke of ±10 mm, which can change the external quality factor (Q_{in}) by an order of 10^2. The RF and radiation interlock, data acquisition, excepting the thermometer and RF circuit, and driving of the coupler were implemented on a programmable logic controller (PLC). The validity of the new test stand at RIKEN was confirmed by comparing the test results of the second prototype carried out in RIKEN and KEK. After assembly of a bulk SC-QWR, a performance test was carried out sequentially from June 2018 in the same procedure as that given in Ref [14]. All the bulk SC-QWRs were fabricated by November 2018 and tested immediately.

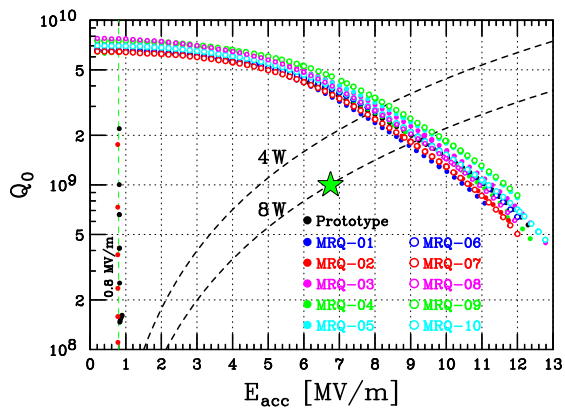

Figure 5: Q_0 vs E_{acc} plot of the bulk SC-QWRs measured at 4.2 K. The green star represents the criteria of the SRILAC.

Figure 5 shows the quality factor Q_0 plotted against acceleration voltage E_{acc} for all the bulk SC-QWRs. The multipacting phenomena observed at 0.8 MV/m were not serious, and it could be processed within a few hours. The test results indicate very high values of Q_0 and E_{acc} for all SC-QWRs; thus, all the SC-QWRs passed the acceptance test successfully. The maximum E_{acc} is significantly higher than the required value of 6.75 MV/m, and no exponential deterioration of Q_0 was observed for any of the SC-QWRs. The resonant frequency of all the SC-QWRs is in the range of the frequency tuner, as expected. Details of the test results are presented in Ref. [17]. The mechanical vibration was also measured and analyzed as described in Ref [19].

After the performance test, the SC-QWR was slowly leaked in an ISO class 1 clean room (also KOKEN floor KOACH) at RIKEN. The test couplers and vacuum exhaust pipes were removed from the SC-QWRs and blank flanges

ISBN: 978-3-95450-211-0 doi:10.18429/JACoW-SRF2019-TUP037

were attached, and the units were sent back to the factory for the post-process of installing the magnetic shield and titanium jacket. Performance tests were performed on four of the SC-QWRs after attaching the jackets. X-rays were observed and the Q_0 values dropped at around 5.2 MV/m for two of the SC-QWRs. It is considered that particles were mixed in the SC-QWR during the slow leak procedure. The two other SC-QWRs were found to be fine. The remaining six SC-QWRs were not tested due to budgetary schedule limitations. Therefore, the steps after HPR were carried out again for eight of the ten SC-QWRs except for two fine SC-QWRs.

Fundamental Power Coupler

The input power coupler for the SRILAC [20] is a coaxial type with a WX-39D connection plug, which has a single disc-shaped ceramic window. The ceramic window is made of KYOCERA A479B with a TiN coating on the vacuum side and is located in the RT part of the coupler. The inner conductor is an oxygen-free copper solid material without forced cooling. The outer conductor is copper plated on the inner surface of a thin stainless steel, where the RRR variation of the copper due to the plating thickness was taken into account to minimize heat penetration. The coupler was designed to handle RF input powers greater than 5 kW CW. By changing the insertion distance of its antenna, the coupling can be adjusted so that the external quality factor Q_{ext} can be varied from 1×10^6 to 4.5×10^6.

A pair of couplers were mounted on a conditioning resonator in the ISO class 1 clean room at RIKEN and conditioned with a 5 kW RF power CW. The conditioning was performed by inputting the RF power from one coupler and extracting it from the other coupler, and the RF power was terminated by a dummy load. The vacuum level and the detection output of an arc sensor were used for interlocking with the RF amplifier to gradually increase the RF input power. The conditioning was completed successfully for all 10 couplers without any difficulty.

Cryomodule Assembly and Installation

The design of the SRILAC cryomodule [21] is based on the first prototype cryomodule. CM1 and CM2 contain four SC-QWRs, while CM3 is half the size of CM1 and CM2. All the cold masses are mounted on the base plate by G10 pillars for thermal insulation. The SC-QWRs are supported together at a point in consideration of the movement by heat contraction. The thermal shield is made of aluminum and cooled with liquid nitrogen. Two Gifford–McMahon cryocoolers (SHI CH-110LT) with a cooling power of 100 W at 40 K are also attached to the thermal shield for operation without liquid nitrogen. The cryocoolers are directly supported on the floor by an independent stand as a measure against their vibration. A bellows is inserted between the cryocooler and cryomodule, and the cryocooler head is connected to the thermal shield via copper braided wires. CERNOX, PtCo, and Pt100 thermometers are attached to the SC-QWRs, thermal shields, thermal anchors, pipings, etc. The vacuum vessel of the cryomodule is made of carbon steel with electroless nickel plating to shield the external magnetic field.

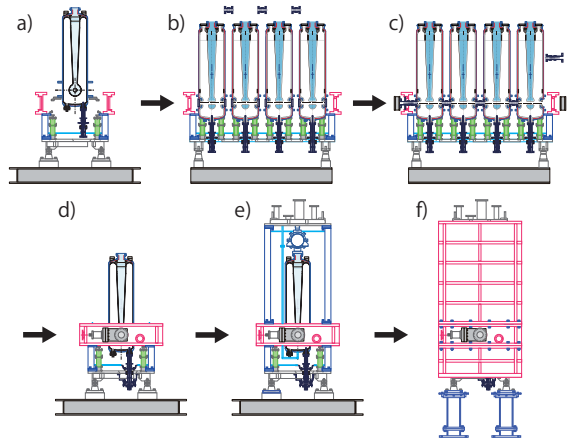

Figure 6: Assembly procedure of SRILAC cryomodules.

Figure 6 shows the assembly procedure of the cryomodules. Because there was no crane in the ISO class 1 clean room, we used a class 8 semi-clean room for the assembly, except for the work of releasing the beam vacuum. A trial-and-error process was performed for CM2, the first assembled module, and the procedure was changed a little for the other cryomodules. The procedure that was finally settled on was as follows. First, the base plate and middle body were mounted on an assembly truck in the semi-clean room, and the support pillars and bottom thermal shield were attached. Each SC-QWR with the coupler attached was mounted on the top, as shown in Fig. 6(a), and roughly aligned. The whole truck was carried to the ISO class 1 clean room, and the bellows between the SC-QWRs were assembled (Fig. 6(b)). The beam pipes, gate valves, and the vacuum exhaust line of SC-QWRs were attached (Fig. 6(c)), and a vacuum leak test was performed. The whole truck was taken to the semi-clean room and the SC-QWRs were aligned. The frequency tuners, lower cryo-pipings, cryocoolers, thermometers, etc., were installed (Fig. 6(d)). The piping, etc., were then attached to the top plate and the top plate was mounted on the cryomodule assembly (Fig. 6(e)). After connecting the helium line, a leak test of the helium line was performed. We then performed the inspection for compliance with safety regulations. The lower thermal shield, thermal anchors, and super insulators were installed, and the cryomodule assembly was transported from the clean room to the installation site. The nitrogen line and upper thermal shield were assembled, and instrumentation such as thermometers and liquid level gauges were attached. The upper vacuum vessel was mounted on the cryomodule assembly as shown in Fig. 6(f) and a safety valve, rupture disc, etc., were attached on the top of the cryomodule. Finally, inspection of the outer piping was undertaken and the cryomodule assembly work was completed.

Figure 7 shows photographs during the assembly and installation of the cryomodule. The three cryomodules were

ISBN: 978-3-95450-211-0 doi:10.18429/JACoW-SRF2019-TUP037

completed and installed in early March 2019. The installation of vacuum pumping system is now in progress in situ using a local clean booth, as shown in Fig. 7(f). A new slow-leak and slow-pumping system using mass-flow controllers has been developed and introduced to the local clean work.

Figure 7: Photographs of cryomodule assembly in the ISO class 1 clean room (a) and semi-clean room (b), transportation from the clean room to the installation site (c), installation of CM2 (d), installation of SRILAC cryomodules (e), and clean work in situ (f).

Other Components

All the cryomodule related measurements, vacuum pumps, heaters, and interlocks are controlled by a duplicated PLC. The LLRFs, RF amplifiers, and frequency tuners are also controlled by other PLCs for each cryomodule. The low-level RF controller of the SRILAC is based on a digital feedback module developed on the prototype system [21]. The FPGA used was changed from an XILINX XC6SLX75 to an XC6SLX150. Ten RF amplifiers with maximum output powers of 7.5 kW CW were manufactured for the SC-QWRs for an operational bandwidth of ±60 Hz. These RF amplifiers have built-in isolators and can withstand 7.5 kW reflection without an external circuit. The control panels including the PLCs, LLRFs, and RF amplifiers were built and installed by March 2019.

An RT quadrupole doublet with a steerer function and a vacuum pump are installed at each beam transport connecting the cryomodules. The quadrupole magnets and power supplies are different from those used in the original booster linac. Remodeling of the power supplies, wiring work to the quadrupole magnets installations, and the main cooling water pipe have already been completed.

A beam energy and position monitor (BEPM) of a diagonal cut type is installed in each quadrupole magnet. A total of 11 BEPMs have been manufactured, and 10 units have been mapped with the cooperation of the J-PARC facility. According to the mapping results, the electrodes are manufactured with an accuracy of 50 μm or less in 10 of the BEPMs.

A differential pumping system was proposed and developed to connect the particulate RT section and SRILAC cryomodule. The system is almost complete and good performance is being obtained as described in Ref. [22].

HELIUM REFRIGERATOR

The helium refrigerator of the SRILAC is a HELIAL MF produced by Air Liquide, with a cooling power of 600 W at 4.5 K without liquid nitrogen. It is possible to upgrade the cooling power to 720 W at 4.5 K by flowing liquid nitrogen. Liquid helium is supplied to each cryomodule through a transfer line installed as shown in Fig. 1 via a joint box next to the refrigerator. A valve box located next to each cryomodule has three valves produced by WEKA, used for precooling, helium supply, and helium return. The valve box and cryomodule are connected by five transfer tubes for precooling, helium supply, helium return, nitrogen supply for the shield, and nitrogen return for the shield.

The operation pressure for the SRILAC cryomodule is set to 0.125 MPa and the pressure is controlled by a supply valve so as to not affect the operation of the SC-QWRs. An upright 50 m^3 buffer tank was newly installed to store helium gas. The existing MAYEKAWA screw compressor was diverted for the SRILAC, which had a flow capacity of 74.2 g/s with 1.7 MPa pressure. Because the compressor was installed in another building, piping work was carried out over 200 m to a cold box. Installation and testing of the refrigerator system were completed by March 2019 and passed the completion inspection required by the High-Pressure Gas Safety Act, including the whole SRILAC.

OUTLOOK

Currently wiring work from the control system to each cryomodule is underway. We will test the control program after the wiring work is completed, and the first cooling-down test of the cryomodules will be performed in September. If the cooling-down test is successful, we will connect the beam ducts and BEPMs between the cryomodules and install a differential pumping system. The quadrupole magnets will be installed in November and a beam acceleration test will be performed in December. We are aiming to have the SRILAC ready for experiments from January next year.

ACKNOWLEDGEMENTS

Development of the first prototype system was funded by the ImPACT Program of the Japan Council for Science, Technology, and Innovation (Cabinet Office, Government of Japan). The authors are grateful to Dr. A. Kasugai at QST Rokkasho and Prof. K. Saito at FRIB/MSU for technical advice on the design of the cavity and assembly work.

REFERENCES

[1] M. Odera *et al.*, *Nucl. Instr. Meth. A*, vol. 227, p. 187, 1984.

ISBN: 978-3-95450-211-0 doi:10.18429/JACoW-SRF2019-TUP037

[2] O. Kamigaito *et al.*, *Rev. Sci. Instr.*, vol. 70, p. 4523, 1999.

[3] O. Kamigaito *et al.*, *Rev. Sci. Instr.*, vol. 76, p. 013306, 2005.

[4] K. Morita *et al.*, *JPSJ*, vol.73, p. 2593, 2004.

[5] O. Kamigaito *et al.*, "Present Status and Future Plan of RIKEN RI Beam Factory", in *Proc. IPAC'16*, Busan, Korea, May 2016, TUPMR022, p. 1281.

[6] T. Nagatomo *et al.*, "New 28-GHz Superconducting ECR Ion Source for Synthesizing New Super Heavy Elements of Z>118", in *Proc. ECRIS'18*, Catania, Italy, Sep. 2018, TUA3, p. 53.

[7] N. Sakamoto *et al.*, "Construction Status of the Superconducting Linac at the RIKEN Radioactive Isotope Beam Facility", in Proc. *LINAC'18*, Beijing, China, Sep. 2018, WE2A03, p. 620.

[8] Y. Yano, *Nucl. Instr. Meth. B*, vol. 261, p. 1009, 2007.

[9] H. Okuno *et al.*, *Prog. Theor. Exp. Phys.*, vol. 2012, no. 1, p. 03C002, 2012.

[10] K. Yamada *et al.*, "Conceptual Design of SC Linac for RIBF-Upgrade Plan", in *Proc. SRF'13*, Paris, France, Sep. 2013, MOP021, p. 137.

[11] K. Yamada *et al.*, "Design of a New Superconducting Linac for the RIBF Upgrade", in *Proc. LINAC'14*, Geneva, Switzerland, Sep. 2014, THPP118, p. 1127.

[12] N. Sakamoto *et al.*, "Design Studies for Quarter-wave Resonators and Cryomodules for the RIKEN SC-Linac", in *Proc. SRF'15*, Whistler, Canada, Sep. 2015, WEBA06, p. 976.

[13] K. Ozeki *et al.*, "Cryomodule and Power Coupler for RIKEN Superconducting QWR", in *Proc. LINAC'16*, East Lansing, USA, Sep. 2016, p. 598.

[14] K. Yamada *et al.*, "First Vertical Test of Superconducting QWR Prototype at RIKEN", in *Proc. LINAC'16*, East Lansing, USA, Sep. 2016, p. 939.

[15] N. Sakamoto *et al.*, "Construction and Performance Tests of Prototype Quarter-wave Resonator and its Cryomodule at RIKEN", in *Proc. SRF'17*, Lanzhou, China, July 2017, WEYA02, p. 681.

[16] http://www.jst.go.jp/impact/en/program/08.html

[17] K. Suda *et al.*, "Fabrication and Performance of Superconducting Quarter-Wavelength Resonators for SRILAC", presented at the SRF'19, Dresden, Germany, Jun.-Jul. 2019, paper MOP055.

[18] A. Miyamoto *et al.*, "MHI's Production Activities of Superconducting Cavity", in *Proc. SRF'15*, Whistler, Canada, Sep. 2015, THPB029, p. 1141.

[19] O. Kamigaito *et al.*, "Measurement of Mechanical Vibration of SRILAC cavities", presented at the SRF'19, Dresden, Germany, Jun.-Jul. 2019, paper TUP042.

[20] K. Ozeki *et al.*, "Input Power Coupler for SRILAC", *RIKEN Accel. Prog. Rep.*, vol. 52, to be published.

[21] N. Sakamoto *et al.*, "Development of Superconducting Quarter-Wave Resonator and Cryomodule for Low-Beta Ion Accelerators at RIKEN Radioactive Isotope Beam Factory", presented at the SRF'19, Dresden, Germany, Jun.-Jul. 2019, paper WETEB1.

[22] H. Imao *et al.*, "Non-Evaporative Getter-Based Differential Pumping System for SRILAC at RIBF", presented at the SRF'19, Dresden, Germany, Jun.-Jul. 2019, paper TUP013.